Pharm Res (2013) 30:1435–1446
DOI 10.1007/s11095-013-0984-9

RESEARCH PAPER

Efficacy of Aerosolized Celecoxib Encapsulated Nanostructured Lipid Carrier in Non-small Cell Lung Cancer in Combination with Docetaxel

Apurva R. Patel • Mahavir B. Chougule • Townley I. • Ram Patlolla • Guangdi Wang • Mandip Singh

Received: 16 November 2012 / Accepted: 9 January 2013 / Published online: 30 January 2013

ABSTRACT

Purpose Evaluation of *in-vivo* anticancer activity of aerosolized Celecoxib encapsulated Nanolipidcarriers (Cxb-NLC) as a single therapeutic agent and combined with intravenously administered Docetaxel (Doc) against non-small cell lung cancer.

Methods Cxb-NLC were prepared by high-pressure homogenization and were characterized for its physicochemical characteristics. Metastatic A549 tumor model in Nu/Nu mice was used to evaluate response of aerosolized Cxb-NLC & Doc. Isolated lung tumor samples were analyzed for: a) DNA fragmentation and cleaved caspase-3 by immunohistochemistry, b) apoptotic and angiogenic protein markers by western blot, c) global proteomic alterations by an isobaric labeling quantitative proteomic method and d) toxicity studies of NLC.

Results The particle size of Cxb-NLC was 217 ± 20 nm, while entrapment efficiency was more than 90%. Cxb-NLC and Doc alone and in combination showed 25 ± 4%, 37 ± 5%, and 67 ± 4% reduction in tumor size respectively compared to control. Proteomic analysis with combination treatment further revealed significantly decreased expression of multiple pro-survival and pro-metastasis proteins as well as tumor invasion markers and the expression of S100 family proteins, such as S100A6 and S100P were decreased by 2.5 and 1.6 fold.

Conclusions Combination therapy with Cxb-NLC and Doc showed significant reduction in tumor growth which was further confirmed by proteomic analysis.

KEY WORDS celecoxib · inhalation delivery · lipid nanoparticles · lung targeting · nanoparticles toxicity

INTRODUCTION

Lung is a mostly common site of primary malignancy for metastasis from other primary tumors such colon, breast, prostate, *etc*. Despite advances in lung cancer treatment, effectiveness of anticancer treatment is relatively low in non-small cell lung cancer (NSCLC) patients (1). Non-localized drug delivery has low success rate and poor clinical outcome because of a sub-therapeutic concentration of therapeutic agent reaches the desired site of action. Also, most of the chemotherapeutic drugs administered by conventional route (*i.e.* oral or parenteral) also exert the cytotoxic effect on normal healthy cells inhibiting their growth and thereby resulting in toxic adverse effects (2). Because of its advantages localized inhalation drug delivery has generated interest among scientists as a strategy to achieve better activity of chemotherapeutic drugs for treatment of lung cancer (3).

Cyclooxygenase-2 enzyme is responsible for the progression and growth of NSCLC and is also found to be up-regulated among various cancers (4,5). Docetaxel (Doc) has been approved by FDA for NSCLC therapy. Several studies have

Electronic supplementary material The online version of this article (doi:10.1007/s11095-013-0984-9) contains supplementary material, which is available to authorized users.

A. R. Patel · R. Patlolla · M. Singh (✉)
College of Pharmacy and Pharmaceutical Sciences
Florida A&M University, Tallahassee, Florida 32307, USA
e-mail: mandip.sachdeva@famu.edu

M. B. Chougule (✉)
Department of Pharmaceutical Sciences, College of Pharmacy
University of Hawaii at Hilo Hilo, Hawaii 96720, USA
e-mail: mahavir@hawaii.edu

T. I. · G. Wang
Department of Chemistry, Xavier University of Louisiana
New Orleans, Los Angeles 70125, USA

shown that the Doc combined with other anticancer agents, improved anticancer activity compared to Doc alone in the lung cancer treatment (5–8). The aerosolized celecoxib (Cxb) solution at 4.56 mg•kg^{-1}•day^{-1} has been shown to exert synergistic anticancer activity (61% tumor size reduction) when used in combination with anticancer agents such as docetaxel (Doc) (9). However, the aerosolized Cxb solution at 4.56 mg•kg^{-1}•day^{-1} showed non-significant anticancer activity similar to that of orally administered Cxb solution at 150 mg•kg^{-1}•day^{-1}. We have investigated the pharmacokinetic parameters of aerosolized Cxb solution at 4.82 mg•kg^{-1}•day^{-1} to elucidate the Cxb concentration in lung tissues in Balb/c mice (10). We have found that the non-siginificant ($p<0.01$) anticancer activity of aerosolized solution was a result of faster clearance of Cxb from lung tissues. The aerosolized Cxb solution was cleared faster from the lungs with 4.9% of administered Cxb was retained in the lungs after 6 h of nebulization and at 12 h, Cxb concentrations were below the detection limits in lung tissue. Our pharmacokinetic results with aerosolized Cxb solution demonstrated a need for increasing the lung residence time of Cxb in order to explore its anticancer potential.

Excipients are commonly used to stabilize the formulations of hydrophobic agents and frequent use of these excipients (surfactants & co-solvents) causes inflammation in lungs (11). Encapsulation of hydrophobic compounds within nanoparticles imparts the stability to drug against degradation and allows prolonged release of the encapsulated drug in a controlled manner (12,13). This will increase the lung residence time of drug as well as enhanced anticancer activity compared to drug solution. The nanostructured lipid carriers (NLC) has been explored for delivery of hydrophobic therapeutic agent (12). NLC are made of solid outer layer entrapping oil core, which allows higher payload of lipophilic drugs (14). Considering the faster clearance of aerosolized Cxb solution from lungs we have prepared Cxb-NLC in order to enhance the lung residence time of Cxb. Our earlier studies demonstrated that encapsulation of Cxb (a lipophilic COX-2 inhibitor) in the NLC and aerosolized delivery of Cxb-NLC (1.47 mg•kg-1•day-1) resulted in the enhanced lung residence time compared to the solution formulation (10). The plasma concentration *vs* time profile of aerosolized Cxb-NLC showed 4 fold higher AUC at 4 fold reduced dose of Cxb compared to aerosolized Cxb solution, which warrants further evaluation of *in vivo* effectiveness of Cxb-NLC in an lung cancer tumor model. Therefore, we hypothesize that the increase in the lung residence time of Cxb using aerosolized delivery of Cxb-NLC will significantly inhibit the NSCLC tumor growth *in-vivo* as a single therapeutic agent and combined with Doc. Our approach of using aerosolized delivery of Cxb-NLC will overcome the limitation associated with Cxb solution by significantly increasing the Cxb lung residence time and will inhibit the lung tumor growth.

Our earlier studies with aerosolized Cxb solution in combination with Doc has utilized an orthotopic lung cancer xenograft model (9). In the current study, we evaluated Cxb-NLC as a novel carrier system for *in-vivo* anticancer activity in lung tumor metastasis model using Nu/Nu mice and investigated the underlying mechanism of action using Western blotting, immunohistochemical techniques and proteomic analysis. The evaluation of anticancer activity of aerosolized Cxb-NLC as a single therapeutic agent and combined with Doc in the lung tumor metastasis model and proteomic evaluation will elucidate the effectiveness of our approach and help to further identify suitable targets. Furthermore, we have also determined the toxicity profile of inhaled Cxb-NLC in healthy Balb/C mice using tissue myeloperoxidase (MPO) activity measurement to assess the safety of nanoparticles.

MATERIALS AND METHODS

Materials

Doc and Cxb were given by Sanofi-Aventis (Pennsylvania, USA) and Pfizer Inc. (Illinois, USA), respectively. MCT oil (Miglyol 812N) and Glycerol dibehenate EP-glyceryl behenate NF (Compritol 888 ATO) were free samples from Sasol GmbH (Witten, Germany) and Gattefosse (Saint Priest, France). All other material or chemicals were analytical grade and purchased from VWR international, USA. NSCLC cell line A 549 was purchased from American Type Culture Collection (Rockville, MD) and were cultivated in F12K medium supplemented with 10% fetal bovine serum and antibiotic mix PSN (Gibco® Invitrogen, USA) containing Penicillin, Streptomycin and Neomycin.

Animals

Nu/nu mice (4–6 weeks old) for anticancer activity studies and Balb/c mice (4–6 weeks old) for the NLC lung toxicity studies were purchased from Charles River Laboratories. The animal protocol was approved by Institutional Animal Care and Use Committee (IACUC) of Florida A&M University. Before starting the experiments, animals were housed in controlled environment (25 ± 1°C & 40–60% humidity) for 1 week. To acclimatize animals for inhalation studies and to prevent any discomfort during experiments, animals were trained for 4–5 days prior to start of experiment by nebulizing water for 30 min.

NLC Preparation and Characterization

Cxb-NLC were made using Cxb, Compritol (solid lipid), Miglyol (liquid lipid) and sodium taurocholate (surfactant)

by hot melt homogenization technique as described previously (12). Blank NLC (without drug) were used as control for comparison. The physicochemical properties such as size, charge of NLC were analyzed with Nicomp Particle sizer (USA). An drug assay and percent drug entrapped were analyzed as described previous (10).

Effectiveness of Cxb-NLC and Doc Against A549 Cells

Effect of Cxb-NLC in combination with Doc against A549 cell line was measured as mentioned earlier literature (15). In brief, the A549 cancer cells were cultured in 96-well plates (10^4 cells/well) and incubated with different treatment groups for different time points. Doc in the range of 0.20–52.0 nM was used with or without presence of Cxb solution or Cxb-NLC (6 and 12 μM). The plates were incubated at 37±0.2°C and cell viability was determined at 48 and 72 h by crystal violet assay (15). The isobolographic analysis was used to measure the extent of interactions of Doc combined with Cxb (Cxb solution and Cxb-NLC) (16). The combination index (CI) values were calculated based on IC_{50} values as described previously (15).

Anticancer Activity of Aerosolized Cxb-NLC

The A549 cells (2 million cells/mice) were injected to the Nu/nu mice *via* tail vein to develop the lung metastatic tumor model. A pilot study showed that lung tumors were developed after 1–2 weeks of tumor cell injection. Ten days post cancer cell inoculation, the animals were randomly grouped into four groups. The mice were grouped (n=8) and treated with i) aerosolized blank NLC, ii) i.v. Doc, iii) aerosolized Cxb-NLC, and iv) aerosolized Cxb-NLC + i.v. Doc. Cxb-NLC was given to mice (30 min exposure/day) by nebulization for up to 28 days (17). The i.v. Doc treatment at 10 mg•kg^{-1} was administered to mice on 14th, 18th, and 22nd post tumor inoculation days (17). Cxb-NLC were nebulized for 30 min using Inexpose™ (SCIREQ Scientific Respiratory Equipment Inc, Montreal, QC) as described previously (17). Mice were euthanized and lung tumor tissues were collected at end of the study. Therapeutic activity of aerosolized Cxb-NLC as a single therapeutic agent and combined with Doc were evaluated in terms of tumor weight and volume. Tumor tissues were fixed in formalin for immunohistochemistry (IHC), TUNEL, Hematoxylin & Eosin staining and for western blotting tissues were stored in −80°C.

Western Blot Analysis of Tumor Tissues

Tumor tissues were processed and western blot analysis was perfomed as per previously described method (17). Briefly, RIPA buffer with protease inhibitor cocktail was used to extract proteins. Proteins (50 μg) were subjected to SDS-PAGE and immunoblotting. The blots were incubated with different antibodies, such as Bax (1:500), cleaved caspase-3 (1:500), Bcl-2 (1:500), vimentin (1:500), caspase-9 (1:500) and β-actin (1:500). Primary antibodies incubation was followed with HRP conjugated secondary antibodies (1:1000) using chemiluminescent reagent (Pierce, Rockford, IL) and X-ray film development. Expressions of different protein were measured using ImageJ software (v1.33u, NIH, USA).

TUNEL Assay and Immunohistochemistry (IHC) for Cleaved Caspase-3

TUNEL assay was performed according to manufacturers protocol using DeadEnd™ Colorimetric Assay kit (Promega, Madison, WI) (17) on paraffinized tumor tissue sections. Similarly, the manufacturers recommended protocol was followed using SignalStain™ Cleaved Caspase-3 (Asp 175) IHC Cell Signaling assay kit (Beverly, MA) (17) for IHC. Microscopic analysis was performed using digital camera (DP71, Olympus Center Valley, PA, USA) connected to an Olympus IX71 microscope. Positive staining was recognized as brown staining.

Protein Lysis and Purification

Protein lysates were generated by RIPA lysis buffer (50 μL, PBS pH7.4, 0.1%w/v SDS, 0.25%w/v sodium deoxycholate) containing EDTA-free protease inhibitor and phosphatase inhibitor. Samples were sonicated for 20 s on ice using a Status US70 sonicating probe (Philips Harris Scientific, U.K.) followed by centrifugation (13,400 rpm for duration of 20 min; 4°C) and the resultant liquid phase extracted to new tubes. Urea lysis buffer (50 μL, 7 M urea; 2 M thiourea; 4%w/v CHAPS; 50 mM DTT in PBS) containing EDTA-free protease inhibitor and phosphatase inhibitor (ThermoFisher) was mixed with the pellet and incubated for 30 min with constant vortexing. The samples were sonicated and centrifuged as described above. The liquid phase was extracted and combined with the RIPA buffer protein extract. The urea lysis step was then repeated on the residual pellet giving a total extract of approximately 150 μL. Bradford assay was performed to estimate protein concentration. Protein lysates were prepared for proteomic analysis by first performing a TCA-DOC/Acetone cleanup procedure. Briefly, lysates were incubated with Na deoxycholate (final concentration=0.02%) for 30 min at room temperature. Trichloracetic acid was mixed with a final concentration of 10% and reaction was continued for an additional 2 h. Reactions were then centrifuged to pellet proteins. Pellets were air-dried and then ice-cold acetone was added, reaction was mixed and incubated at −20°C for 12 h. Reactions were then spun at max speed in a microfuge at 4°C for 10 min. Pellets were re-suspended in a modified RIPA

buffer (50 mM Tris; pH 7.2; 150 mM NaCl; 2 mM EDTA; 1.0% Triton X-100; 1.0% Na deoxycholate; 0.1% SDS, 1 mM Phenylmethanesulfonyl fluoride, 1× Halt Protease and Phosphatase Inhibitor). The protein concentrations were measured by BCA assay.

Tandem Mass Tags Labeling

Tandem mass tags TMT6 (Thermo Sci.) with different molecular weights (126~131) were used for relative and absolute quantification as isobaric tags. Two 150 ug aliquots of each cleaned up protein lysate was reduced, alkylated and digested with trypsin (sequencing grade) as per protocol from the TMT Isobaric Mass Tagging kit (Thermo Sci. #90060). Samples were labeled for 1 h with TMT6 reagents as follows: Aliquots of 150-µg digested peptides were each labeled with a different isobaric tag. The control samples (two 150-µg aliquots) were labeled with 126 and 127 mass tag; the combination treated samples (two 150-µg aliquots) were labeled with 128 and 129 mass tags; the single agent treated samples (two 150-µg aliquots) were labeled with 130 and 131 mass tags. The hydroxylamine (5%) was used to stop labeling reaction. The samples were pooled for analysis as: Cxb/control, Dox/Control, Cxb/combo and Dox/combo. Finally the mixed samples were desalted over a C18 SPE column according to the manufacture's direction.

LC-MS/MS Analysis

LTQ-Orbitrap XL instrument (Thermo Scientific, San Jose, CA) was attached to an Ultimate 3000 Dionex nanoflow LC system (Dionex, Sunnyvale, CA) for analysis of peptides as mentioned earlier (18,19). Briefly, peptide detection was carried out at high mass resolution and for reporter ion quantification high energy collision dissociation was employed. Samples were processed for concentration and desalting and peptides were eluted from the analytical column using trap cartridge. Six MS/MS scans (centroid mode) were performed following full MS scan (profile mode) at 60,000 resolving power and three most copious molecular ions were dynamically selected and fragmented. Monoisotopic precursor selection, Charge state screening, FT master scan preview mode and Charge state rejection were enabled for selection of only 2+, 3+ and 4+ ions and they were fragmented by CID and high energy collision dissociation. Database search and TMT quantification was carried out as mentioned in literatures (18,19)

NLC Lung Toxicity

The normal Balb/c mice were given blank NLC and Cxb-NLC for 30 min using Pary LC star nebulizer as described earlier (10). The mice were given NLC each day for 28 days and animals were euthanized at 24 h following of final day of exposure. Neutral buffered formalin (10%v/v) was used to fix the tissues and processed for sectioning. Tissue sections were processed for hematoxylin and eosin staining. Further lung toxicity was evaluated by; 1) acute lung injury assay: To evaluate the edema of lungs, the lung tissues were dried at 60°C for 48 h and wet to dry lung weight ratio was determined; 2) myeloperoxidase (MPO) assay: The myeloperoxidase activity marker was determined using reported method (20,21) to estimate the neutrophil count in the lung parenchyma. In brief, the normal and NLC treated lungs were homogenized. The tissues were centrifuged and pellets were re-suspended in HETAB solution. A 0.1 ml aliquot of sample and 2.9 ml MPO assay reagent were mixed and absorbance was measured at 460 nm using Tecan® infinite m200 spectrophotometer (Tecan, USA). The MPO activity was calculated.

Statistical Analysis

The significance of difference in treatment groups was determined using one-way ANOVA and Tukey's Multiple Comparison Test using GraphPad prism version 5.0 (San Diego, CA), where value of $p < 0.05$ between the groups was considered as statistically significant difference between these groups. Proteomics statistical analysis was performed in Excel (Microsoft, Redmond, WA) to determine significantly altered proteins. Two parameters determined significance, 1) p-value of <0.05 and 2) the ratio value. For all the ratios in the control sample the standard deviation (SD) was determined and then significance was defined as (+/− 2*SD) (22–24).

RESULTS

Nanoparticles (NLC) Characterization

Inhalable Cxb-NLC nanoparticles were prepared using triglycerides. The size and polydispersity of Cxb-NLC was found to be 211±22 nm and 0.22, respectively. The net charge on blank NLC was − 27.38 mV, whereas, Cxb-NLC had −25.30 mV. Cxb content was approximately 1.8 mg/ml with entrapment efficiency (EE) of 95.6% and drug loading of 4% w/w. To determine the aerodynamic properties of Cxb-NLC the Anderson Mark-II cascade impactor was used and "Fine Particle Fraction" (FPF), "Mass Median Aerodynamic Diameter" (MMAD) and "Geometric Standard Deviation" (GSD) were found to be 76.2±5.1%, 1.58±0.14 µm and 1.26±0.32, respectively. Dv50 of 2.71 µm and FPF of 81.12±0.73% indicate that more than 75% of aerosolized Cxb-NLC were below 5 µm indicating the

optimal aerodynamic properties of Cxb-NLC that required for inhalation delivery (25).

Effect of Cxb-NLC on A549 Cells

The IC_{50} values of Cxb-NLC were 252.02 (± 29.6) μg/ml at 24 h; 102.31 (± 5.4) μg/ml at 48 h; and 27.36 (± 2.2) μg/ml at 72 h. IC_{50} values for Doc were 0.036 (± 0.005) μg/ml at 24 h, 0.028 (± 0.004) μg/ml at 48 h and 0.015 (± 0.004) μg/ml at 72 h. The isobolographic analysis was used to see the effect of Doc and Cxb-NLC combination on cell proliferation. Figure 1 shows the isobologram of the interaction between Doc and Cxb-NLC in A549 NSCLC cell line. The Cxb-NLC and Doc combination showed CI values of 0.63 at 48 h and 0.72 at 72 h of treatment which suggests the moderate synergistic activity.

Effect of Aerosolized Cxb-NLC Against A549 Metastatic Tumors

Treatment was given starting 10 days after tumor inoculation for 28 days. Figure 2 show the therapeutic effectiveness to the treatment by changes in tumor weight and volume. Mice treated with Cxb-NLC + Doc and Doc i.v. showed significantly lower lung weight than untreated animals. There were 25 ± 4%, 37 ± 5%, and 67 ± 4% decrease in the tumor volume following Cxb-NLC, Doc i.v. and Cxb-NLC+Doc i.v. treated mice respectively compared to control. Figure 1c shows the non-significant decrease ($p > 0.05$) in body weight of mice treated with Cxb-NLC, Cxb-NLC+Doc and Doc i.v. compare to control.

Effect on Pro-apoptotic, Angiogenic and Cell Survival Proteins

The mechanism responsible for the effect of Cxb-NLC as a single therapeutic agent and combined with Doc, we evaluated several angiogenic, survival, growth inhibitory and apoptotic proteins in tumor lysates (Fig. 3). Cxb-NLC treatments significantly ($P < 0.001$) down regulated Bcl-2 and up regulated Bax, cleaved caspase-9, and cleaved caspase-3 expression compared to the control group (Fig. 3). The Bax/Bcl-2 ratio was increased to 1.5 with Cxb-NLC treated tumors compare to control. Cxb-NLC + Doc treatment significantly increased expression of Bax, cleaved caspase-9, cleaved caspase-3 proteins and decreased expression of Bcl-2 compared to Cxb-NLC and Doc alone treated group. Cxb-NLC, Doc and combination treatment reduced VEGF expression in regressed tumor by 0.27, 0.44 and 0.65 fold, respectively, compared to control (Fig. 3). The expression of survivin protein was also significantly reduced by 0.63 fold (*, $P < 0.01$) and 0.42 fold (*, $P < 0.05$) with Cxb-NLC+ Doc and Doc alone treatment compared to control (Fig. 3).

TUNEL Assay and Immunohistochemistry (IHC) for Cleaved Caspase-3

TUNEL assay showed that apoptosis was negligible in untreated tumors compare to treated with Cxb NLC, Cxb-NLC + Doc (Fig. 4). The Cxb-NLC + Doc treatment showed a significantly higher number of apoptotic cells compared to Doc treatment. The specific cleaved caspase-3 activity in tumors treated with Cxb-NLC, Doc and Cxb-NLC + Doc were significantly higher than untreated control ($P < 0.001$). Furthermore, combination showed higher cleaved caspase-3 activity in A549 tumors compare to single treatment ($P < 0.01$).

Quantitative Proteomic Analysis Reveals Significant Down Regulation of Multiple Proteins in Cxb-NLC and Doc Treated Lung Cancer Tissues

To further investigate the mechanisms of Cxb-NLC and Doc action against lung cancer we performed global

a

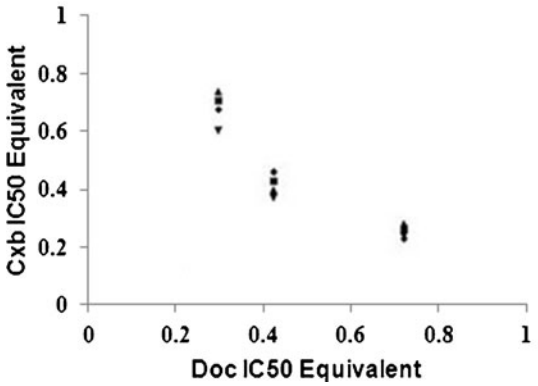

b

Combination	A549 cells	
	Combination Index	Interpretation
Cxb-Soln (6 μg/ml) + Doc	0.46 ± 0.05	Synergism
Cxb-Soln (12 μg/ml) + Doc	0.65 ± 0.03	Moderate Synergism
Cxb-NLC (6 μg/ml) + Doc	0.63 ± 0.08	Moderate Synergism
Cxb-NLC (12 μg/ml) + Doc	0.70 ± 0.08	Moderate Synergism

Fig. 1 Isobolograms (**a**) and (**b**) Combination Index (CI) values of the interaction between Cxb with Doc against human lung cancer cells. Different concentrations of Cxb were employed to study the effect on IC50 of Doc. Variable ratios of drug concentrations and mutually non-exclusive equations were used to determine the CI. The CI values represent mean of four experiments. CI >1.3: antagonism; CI 1.1–1.3: moderate antagonism; CI 0.9–1.1: additive effect; CI 0.8–0.9: slight synergism; CI 0.6–0.8: moderate synergism; CI 0.4–0.6: synergism; CI 0.2–0.4: strong synergism.

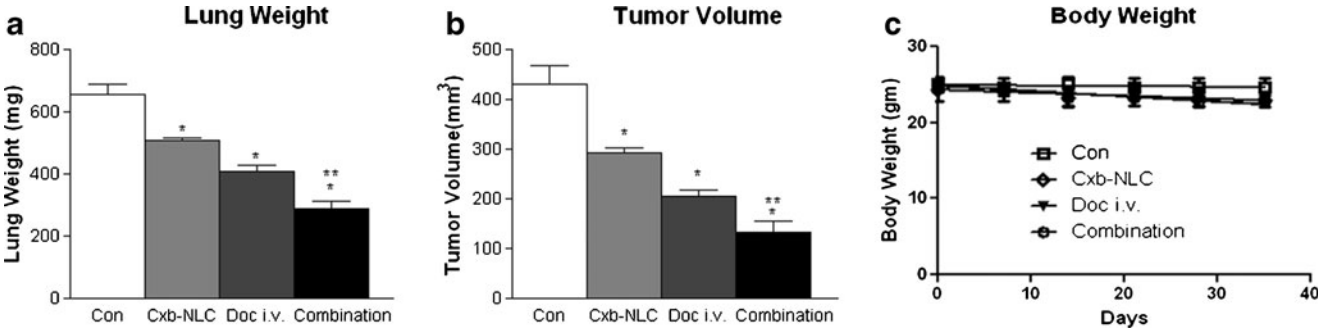

Fig. 2 Effects of Cxb-NLC and Doc on metastatic A549 lung tumor weight (**a**); metastatic A549 lung tumor volume (**b**); mice body weight (**c**). A549 cells (2×10^6) were injected into the nude mice by tail vein. Tumors were established for 7 days before therapy. Tumors from animals treated with Cxb-NLC aerosol (3 times a week), 10 mg/kg Doc (days 14, 18, 22), or combination were harvested after 28 days. Lung weights and tumor volumes were determined for measurement of therapeutic activity of the treatments. One-way ANOVA followed by post Tukey test was used for statistical analysis. $P < 0.05$ (*, significantly different from untreated controls; **, significantly different from single treatments). Data presented are means ± SD ($n = 8$).

proteomic analysis of the drug-treated *vs.* control lung cancer tissues from tumor bearing mice. Three post treatment tumor tissue samples were analyzed: Cxb-NLC treated, Doc treated, and Cxb-NLC+Doc treated. Quantitative data of proteomic fold changes were obtained using a tandem mass tag (TMT) labeling method. The results are summarized in Supplementary Material Tables S1–3 where all identified and quantified proteins are listed with fold changes and statistical significance (p) values. Of particular interests are the proteomic findings of significant downregulation of multiple proteins in both single treatment (Cxb-NLC or Doc) and combination treatment that have been previously implicated in promoting tumor growth and metastasis (Table I). The expressions of seven S100 family proteins were found prominently reduced in all treatments with various degrees of synergy in the combined therapy. For example, the metastasis associated proteins S100A6 (26) and S100P (27,28) were downregulated in the Doc treated lung tumors by 1.6 and 1.2 fold, respectively. After combination treatment, the protein levels went further down by 2.5 and 1.6 fold, respectively, indicating the synergy between Cxb and Doc. The protein anterior gradient 2 (29) was markedly down in tumors treated with Cxb (5 fold, $p = 0.0001$), Doc (2.7 fold, $p = 0.0001$) and Cxb+Doc (5.7 fold, $p = 0.0006$), demonstrating the enhanced anticancer activity of the combo treatment compared to Doc treatment alone. Vimentin, the marker protein of epithelial to mesenchymal transition (EMT) in cancer invasion and metastasis, was seen dramatically downregulated by 3.1, 1.4, and 3.0 fold in Cxb, Doc, and combination treated samples, respectively. Expression levels of other important marker proteins associated with poor prognosis and tumor progression such as trefoil factor 1, galectin-1, and protein DJ-1 were all lowered significantly after treatment with Cxb and Doc either alone or in combination (Table I). To validate proteomic alterations as a result of Cxb-NLC and Doc treatment, we chose vimentin, a hallmark of EMT in cancer progression for Western analysis. As shown in Fig. 3, compared to the control group, vimentin was down-regulated in tumors treated with Cxb-NLC alone ($p < 0.05$), Doc alone ($p < 0.05$), and Cxb-NLC+Doc ($p < 0.05$). Also, vimentin was significantly ($p < 0.05$) down-regulated in combination treatment compared to single agent treatment (Fig. 3). In contrast, Cxb alone or the combination treatment proteomics results showed similar ~3-fold down-regulation of vimentin (Table I). While the vimentin down-regulation results by western blot and proteomic method were varied, the overall trend of decreased expression of vimentin as a result of three treatment strategies was confirmed by these studies.

NLC Lung Toxicity

The safety of the NLC was analyzed based on the lung edema [wet to dry lung weight ratio (WDR)] and inflammatory responses by performing the MPO assay. The WDR of 4.51 ± 0.47 and 4.42 ± 0.29 was found in the non-tumor bearing mice treated with blank NLC and Cxb-NLC. In the tumor bearing mice treated with Cxb-NLC the WDR was 4.67 ± 0.10. The treatment groups showed non-significant ($p > 0.05$) difference in the WDR. Similarly, the MPO activity showed non-significant difference among the different treatment groups. The non-tumor bearing mice treated with Cxb-NLC showed MPO activity value of 98.98 ± 5.52. The MPO activity with non-tumor bearing mice treated with blank NLC and tumor bearing mice treated with blank NLC was found to be 100.24 ± 3.56 and 97.78 ± 3.7, respectively.

DISCUSSION

Localized delivery of anti-cancer drugs directly to the tumor site may be a novel treatment option for patients with lung cancer. Due to increased dose of Cxb (400 mg orally, twice daily) used in phase III clinical trials, patients were showing symptoms of Cxb induced heart attacks and strokes (30). Our previous studied evaluated the anticancer potential of

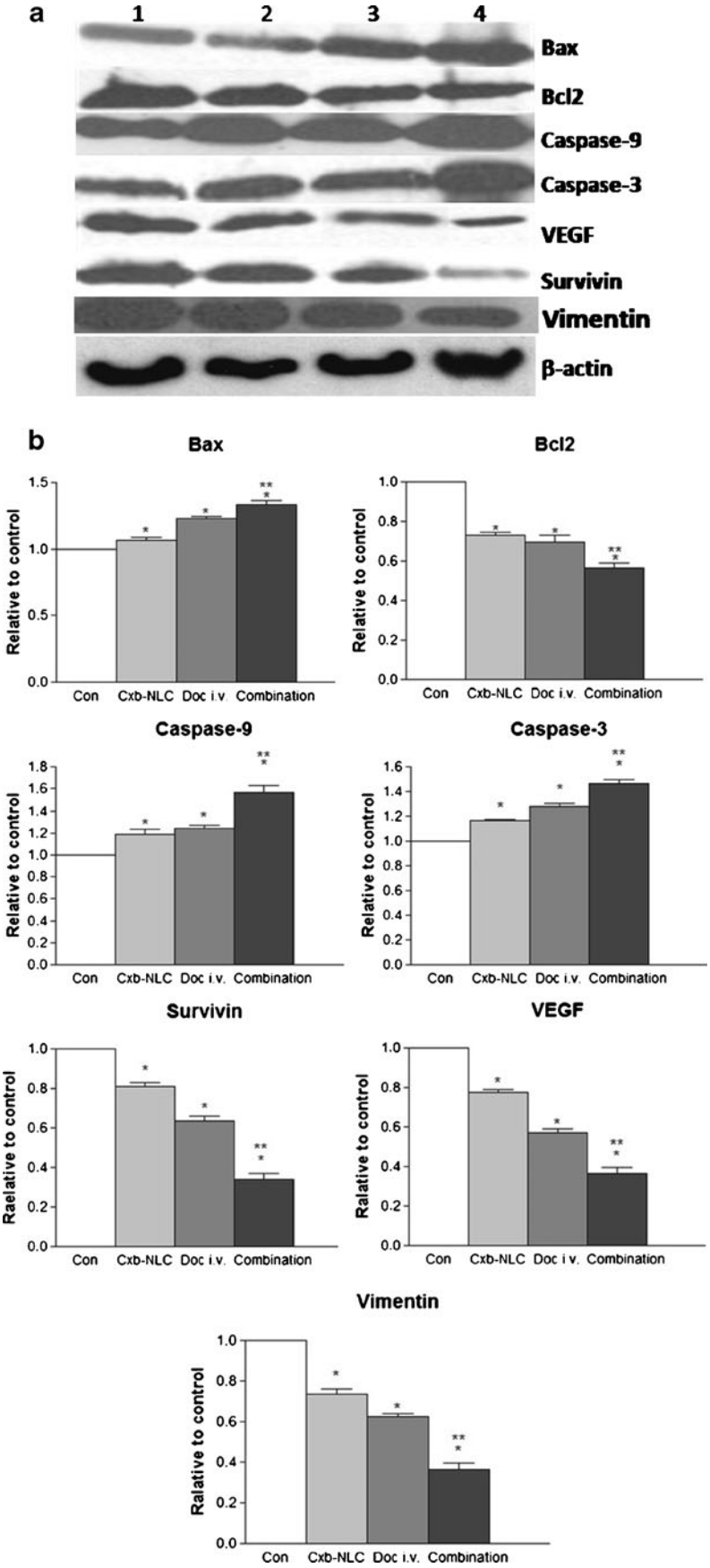

Fig 3 Western blotting of tumor tissue lysates to determine (**a**) expression of Bax, Bcl2, caspase-3, caspase-9, VEGF, Survivin and Vimentin proteins in tumor lysates by western blotting and (**b**) quantitation of apoptotic protein expression. Tumor tissue lysates harvested tumor tissues from control-untreated and treated groups were analyzed by western blotting for protein expressions. Lane 1 = control; Lane 2 = Cxb-NLC; Lane 3 = Doc i.v.; Lane 4 = Cxb-NLC + Doc i.v. Protein expression levels (relative to β-actin) were determined. Mean ± SE for three replicate determinations. One-way ANOVA followed by post Tukey test was used for statistical analysis. $P < 0.01$ (*, significantly different from untreated controls; **, significantly different from single treatments).

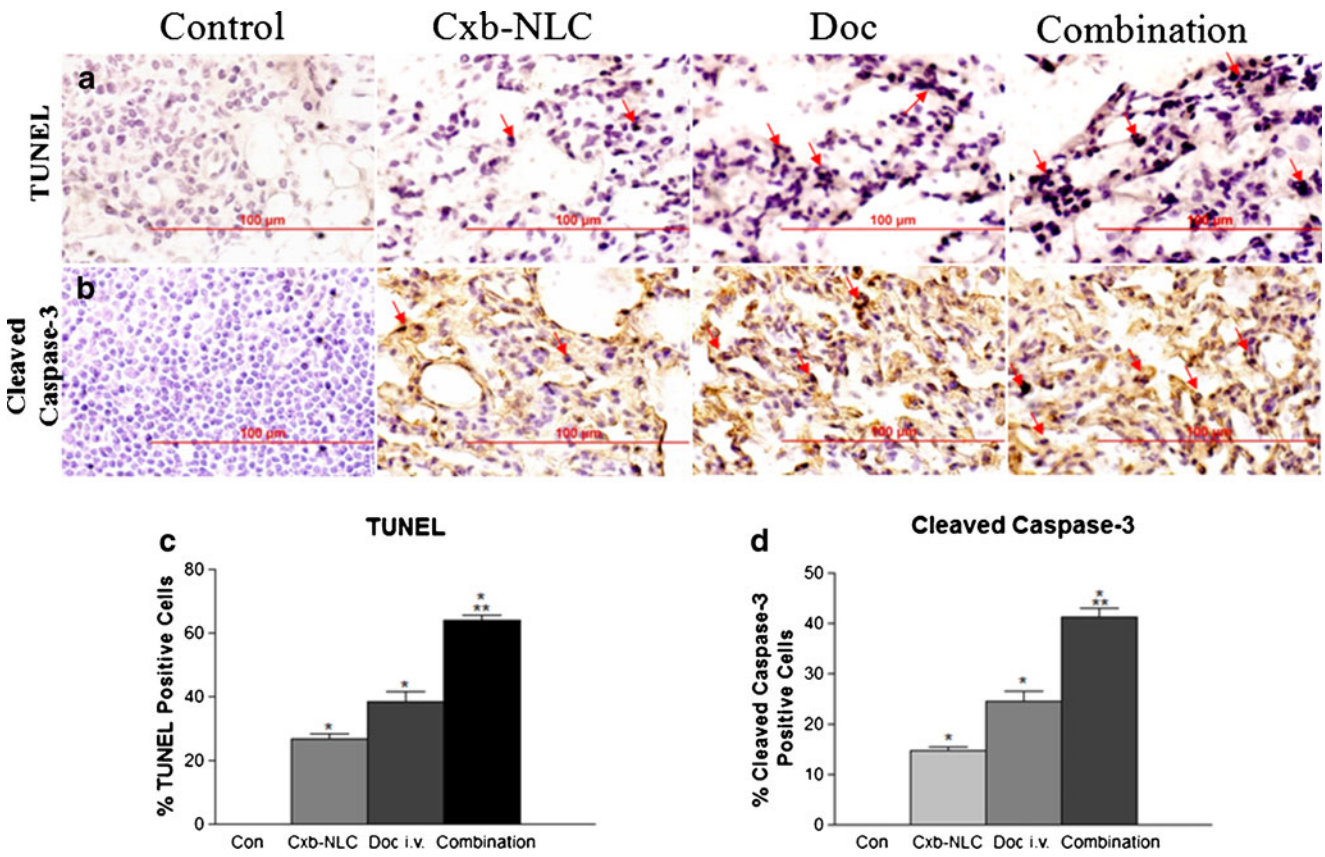

Fig. 4 Immunohistochemical staining of lung tumor tissues for induction of apoptosis using TUNEL assay (**a**); for expression of cleaved caspase-3 (**b**); quantitation of apoptotic cells from TUNEL staining (**c**); and quantitation of caspase-3 positive cells apoptotic cells (**d**). Percentages of TUNEL-positive and cleaved caspase 3-positive cells were quantitated by counting 100 cells from 6 random microscopic fields. Data are expressed as mean+SD ($N=6$). One-way ANOVA followed by post Tukey test was used for statistical analysis to compare control and treated groups. $P<0.01$ (*, significantly different from untreated controls; **, significantly different from single treatments). Original magnification ×40 (Micron bar = 100 μm).

aerosolized Cxb solution at 4.56 mg•kg^{-1}•day^{-1} as a single therapeutic agent and combined with Doc compared to that of orally administered Cxb at 150 mg•kg^{-1}•day^{-1}. We observed that neither aerosolized Cxb solution alone at 4.56 mg•kg^{-1}•day^{-1} nor orally administered Cxb solution alone at 150 mg•kg^{-1}•day^{-1} were effective ($P>0.01$) in inhibition of lung tumor growth (9). However, aerosolized Cxb solution + i.v. Doc showed synergistic anticancer activity (9). The potential of this combination could be further improved if Cxb could be retained in the lungs for longer duration of time. Our pharmacokinetic studies with aerosolized Cxb solution showed that the Cxb was cleared faster from both lung and plasma. Furthermore, the use of aerosolized Cxb-NLC resulted in the increased lung residence time of Cxb compared to aerosolized Cxb Solution (10). Thus, we have investigated the effect of increased lung residence time by aerosolized Cxb-NLC as a single therapeutic agent and combined with Doc on *in vivo* activity in lung tumor metastasis model.

We have evaluated the effectiveness of Cxb-NLC as a single therapeutic agent and combined with Doc *in-vitro* against A549 NSCLC cells. Cxb-NLC formulations showed moderate synergistic effects, whereas Cxb-Solution when given in combination with Doc showed a slight improvement in synergism (CI values of 0.63 at 48 h and 0.72 at 72 h of treatment, respectively). The higher CI index value of Cxb-NLC was due to association of Cxb with the nanoparticles and low amount of free Cxb was available to inhibit the tumor cell growth when given in combination with Doc. Our previous studies strongly support this observation where the IC_{50} values for Cxb-NLC were well correlated with the *in vitro* drug release data (10).

Followed by *in-vitro* analysis of Cxb-NLC + Doc treatment, the efficacy of aerosolized Cxb-NLC as a single therapeutic agent and combined with Doc against A549 metastatic lung tumors were evaluated. In the present study, the aerosolized delivery of Cxb-NLC (1.47 mg•kg^{-1}) combined with Doc (10 mg•kg^{-1}) showed significant ($p<0.01$) reduction in tumor growth compared to the single agent treatment (Fig. 2). The aerosolized Cxb-NLC (1.47 mg•kg^{-1}) alone showed significant ($p<0.01$) inhibition of lung tumor growth compared to control. In contrast, oral Cxb (150 mg•kg^{-1}) and aerosolized Cxb solution (4.87 mg•kg^{-1}) demonstrated a non-significant ($p>0.01$) inhibition of orthotopic lung tumors (9). Cxb-NLC

Table I Significantly Downregulated Proteins in Metastatic Lung Tumors After Treatment of Celecoxib, Docetaxel, or in Combination

Accession	# AAs	MW [kDa]	calc. pI	Description	Fold change **Cxb/Ctrl**	*t*-test (*p* values)	Fold change **Doc/Ctrl**	*t*-test (*p* values)	Fold change **Combo/Ctrl**	*t*-test (*p* values)
IPI00013895	105	11.7	7.12	Protein S100-A11	−2.00	0.001192	−2.06	0.00019	−1.67	0.00504
IPI00016179	98	11.5	6.16	Protein S100-A13	−1.56	0.013084	−1.36	0.00619	−1.74	0.00655
IPI00010214	104	11.7	5.24	Protein S100-A14	−2.06	0.001781	−1.27	0.00924	−1.52	0.01095
IPI00062120	103	11.8	6.79	Protein S100-A16	−2.35	0.000120	−2.98	0.00007	−1.81	0.02407
IPI00032313	101	11.7	6.11	Protein S100-A4	−3.22	0.000637	−2.95	0.00050	−2.47	0.00250
IPI00027463	90	10.2	5.48	Protein S100-A6	−2.14	0.000582	−1.57	0.00132	−2.46	0.00229
IPI00017526	95	10.4	4.88	Protein S100-P	−1.42	0.006295	−1.18	0.11675	−1.59	0.01736
IPI00008527	114	11.5	4.32	60S acidic ribosomal protein P1	−6.33	0.001264	−6.67	0.00181	ND	
IPI00008529	115	11.7	4.54	60S acidic ribosomal protein P2	−1.50	0.000109	−1.32	0.01327	−1.36	0.00631
IPI00942032	175	20.0	9.00	AGR2	−4.95	0.000125	−2.66	0.00014	−5.65	0.00062
IPI00554648	483	53.7	5.59	Keratin, type II cytoskeletal 8	−4.78	0.000106	−2.97	0.00009	−3.52	0.00140
IPI00418471	466	53.6	5.12	Vimentin	−3.09	0.000144	−1.44	0.00003	−3.02	0.00128
IPI00219219	135	14.7	5.50	Galectin-1	−2.82	0.002144	−1.50	0.00012	−1.16	0.05178
IPI00012011	166	18.5	8.09	Cofilin-1	−2.79	0.000365	−1.79	0.00038	−2.05	0.01166
IPI00645674	108	12.5	4.82	Glutathione S-transferase A3	−2.31	0.009014	−1.19	0.03458	ND	
IPI00550363	199	22.4	8.25	Transgelin-2	−2.01	0.000376	−1.32	0.00053	−1.64	0.00419
IPI00022283	84	9.1	4.35	Trefoil factor 1	−1.68	0.005099	−1.91	0.00447	−1.22	0.01276
IPI00015894	356	38.0	5.19	Cdc42 effector protein 4	−1.36	0.041237	−1.14	0.01753	ND	
IPI00298547	189	19.9	6.79	Protein DJ-1	−2.14	0.000770	−1.38	0.00090	−2.01	0.00111
IPI00917753	265	31.0	4.23	SET nuclear oncogene	−3.28	0.000058	−0.99	0.92124	−1.92	0.01838

was found to be highly effective at reduced dose compared to oral Cxb (150 mg•kg^{-1}) and aerosolized Cxb solution (4.87 mg•kg^{-1}) respectively. The enhanced anticancer activity of aerosolized Cxb-NLC compared to aerosolized Cxb solution was very well correlated with increased lung residence time of Cxb as shown in our previous studies (10). The aerosolized Cxb-NLC combined with Doc showed significant reduction of tumor growth compared to that of reported oral Cxb + Doc and aerosolized Cxb solution + Doc treatment. Furthermore, the aerosolized Cxb-NLC, Doc and combination treatment showed non-significant change in weight loss suggesting favorable toxicity profile of Cxb-NLC and Doc at doses used in this study (Fig. 1c). Effectiveness of pulmonary delivery against conventional systemic delivery with various formulations has been showed by various scientists. Such as, Verschraegen *et al.* (31) showed that aerosol administration of liposomal 9-nitro-20(s)-camptothecin (13.3 μg•kg^{-1}•day^{-1}) in primary or metastatic lung cancer patients was effective and safe. In another study with a renal carcinoma lung metastasis model, administration of paclitaxel liposome aerosol resulted in non-significant difference in lung weights ($P > 0.05$) (32). Hirokazu *et al.* (33) showed that inhalation delivery of Chitosan–interferon-β gene complex powder (a dose of 1 μg) in lung metastatic mice model significantly increased survival time of mice compared to control. Zhang *et al.* (34) also showed decreased lung metastases in melanoma mice models following inhalation delivery of 10-Hydroxycamptothecin. Olga B. Garbuzenko *et al.* (35) also effectively delivered doxorubicin liposomes and siRNA by inhalation and showed decrease in tumor cell by 45% compare to control tumor. Also, our study shows that localized delivery of aerosolized Cxb-NLC as a single therapeutic agent and combined with Doc resulted in significant anti-tumor activity at a reduced dose compared to aerosolized Cxb solution and oral Cxb dose (9).

Previous studies has shown the molecular mechanisms involved with the anti-proliferative effect, apoptotic response, inhibition of angiogenesis and alteration of various proteins expression related to the prostaglandins pathway of Cxb with Doc under *in vitro* settings, xenograft A549 tumors, and orthotopic A549 tumors (5,9). In this study, we further elucidated the underlying mechanism of action of Cxb-NLC + Doc treatments. We observed that Cxb-NLC + Doc activated initiator caspases, such as caspase-9 followed by activation of caspase-3. Furthermore, expression level of DNA fragmentation and cleaved caspase-3 was significantly increased in treatments compared to control showing the anticancer activity through

apoptosis (Fig. 4). Our *in vivo* studies showed that Doc, Cxb-NLC, and Cxb-NLC + Doc treatment increased Bax expression and decreased survival (Bcl2) proteins (Fig. 3).

Studies have shown levels of VEGF mRNA and protein levels are associated to COX-2 expression (36,37) and VEGF levels in tumors were found to be down regulated by COX-2 inhibitors (38). Furthermore, we observed that Cxb-NLC + Doc treatment inhibits VEGF (Fig. 3) in tumors compared to single agent and control. The expression of survivin was found to be decreased in the Cxb-NLC, Doc and Cxb-NLC + Doc treatment (Fig. 3). The down-regulation of survivin (negative regulator of apoptosis) expression may result in induction of apoptosis in tumor cells by activation of caspases.

Furthermore, proteomic analysis of the Cxb-NLC and Doc treated lung tumors provided additional support to synergistic actions of these agents. S100 proteins are often upregulated in various solid tumors and are associated with tumor progression (39). The observation of marked down-regulation of these proteins in the treated lung tumor tissues *in vivo* confirms the drug mechanism in suppressing tumor growth and metastasis. Kimura *et al.* showed in patients with NSCLC that S100A4-negative/alpha-catenin-positive expression was responsible for higher survival in patients than S100A4-positive expression (40). Indeed, a recent study revealed that genetic exhaustion of S100A4 results in significant reduction of the metastatic potential in lungs of PyMT-induced mammary tumors (41). Increased expression of S100A11 in NSCLC is related to higher tumor-node-metastasis stage as well as positive lymph node status (42), suggesting that the downregulation of this protein might be an important prognostic marker in monitoring the invasive and metastatic potential of NSCLC patient treated with Doc or combination regiment. The protein S100P has been reported to predict distant metastasis and survival in non-small cell lung cancer (39,43), again confirming the significance of its diminished expression in Cxb-NLC and Doc treated lung tumor tissues.

In addition to the S100 family proteins, other significantly downregulated proteins also provided important evidence to the synergistic drug activity of anti-metastasis and pro-apoptosis. For example, AGR2 is an important tumor biomarker and negative prognostic factor for both hormone dependent and independent cancers including NSCLC (29, 45–47). In our study, AGR2 was one of the most prominently downregulated protein, exhibiting over 5-fold decrease in post combination treatment lung tumor tissues. While the mechanism of AGR2 involvement in mediating tumor invasion and metastasis is not fully understood, our results clearly demonstrate the prognostic value of AGR2 that could be clinically exploited for NSCLC patients undergoing chemotherapy. Another interesting observation was the alteration of protein DJ-1, whose expression was consistently reduced across the three drug-treated tumor samples (Table I). DJ-1 expression was increased compared to paired non-neoplastic lung tissue, and correlated positively with relapse incidence (44). It is believed that DJ-1 is a key negative regulator of PTEN which antagonizes the PI3K signaling pathway and suppresses cell survival. Thus downregulation of DJ-1 leads to decreased phosphorylation of PKB/Akt. Furthermore, some studies showed that Cxb also acts through PI3K/Akt-dependent, survivin and Bcl2 related mechanisms, which may be COX-2-independent. The proteomic analysis was further confirmed with western blot data using vimentin as a model marker which showed a similar profile. Taken together, the proteomic findings of significant downregulation of multiple proteins and Western blot data reflecting decreased expression of survivin, caspase-3, and vimentin suggest that combination treatment leads to tumor remission by suppressing survival signaling, activating apoptotic pathway, and inhibiting EMT. Our proteomic studies suggest that S100, AGR2, and DJ-1 proteins may be explored as viable targets for lung cancer treatment. Further investigation for non-apoptotic signaling pathways involved in anti-cancer activity is in progress to gain more insights.

Even though lipids used in making NLC are biodegradable we do not know safety profile of NLC delivered *via* inhalation, thus we evaluated NLC for its toxicity following anti-tumor activity. The WDR was used to assess lung edema and results showed that aerosolized Cxb-NLC has WDR < 6.5. Where, normal mice have a *WDR* in the range of 4 to 6.5 and in case of severe lung edema a value increases significantly (>6.5) (21,45,46). Hence, it appears that aerosolized Cxb-NLC did not cause any pulmonary edema. Non-significant difference was observed in the MPO activity in non-tumor bearing mice on treatment with blank-NLC and Cxb-NLC showing that the Cxb-NLC did not cause lung inflammation. The tumor bearing mice treated by the Cxb-NLC showed decrease in MPO activity, which may be due to the anti-inflammatory effect of Cxb. These results show that pulmonary delivery Cxb-NLC and NLC are safe to use for localized delivery. In addition, the evaluation of lung tissues at the end of the study period demonstrated normal lung architecture, indicating no significant pulmonary impacts to following particle exposures.

CONCLUSION

In conclusion, this study shows the effectiveness of aerosolized Cxb-NLC + Doc therapy against a murine lung cancer model. The aerosolized Cxb-NLC showed significant inhibition of tumor growth as a result of increase in lung residence time. The therapeutic activity of Doc was improved by aerosolized Cxb-NLC through various mechanisms in lung cancer. Thus the use of aerosolized Cxb-NLC + Doc therapy may be a

promising remedial stratagem for the treatment for lung cancer that allows use of reduced dose resulting in fewer side effects.

ACKNOWLEDGMENTS AND DISCLOSURES

Author acknowledges the financial support provided by NIH RCMI grant 5G12RR026260-03.

REFERENCES

1. Whitehead CM, Earle KA, Fetter J, Xu S, Hartman T, Chan DC, *et al.* Exisulind-induced apoptosis in a non-small cell lung cancer orthotopic lung tumor model augments docetaxel treatment and contributes to increased survival. Mol Cancer Ther. 2003;2 (5):479–88.
2. Sharma S, White D, Imondi AR, Placke ME, Vail DM, Kris MG. Development of inhalational agents for oncologic use. J Clin Oncol. 2001;19(6):1839–47.
3. Labiris NR, Dolovich MB. Pulmonary drug delivery. Part I: physiological factors affecting therapeutic effectiveness of aerosolized medications. Br J Clin Pharmacol. 2003;56(6):588–99.
4. Hida T, Kozaki K, Muramatsu H, Masuda A, Shimizu S, Mitsudomi T, *et al.* Cyclooxygenase-2 inhibitor induces apoptosis and enhances cytotoxicity of various anticancer agents in non-small cell lung cancer cell lines. Clin Cancer Res. 2000;6(5):2006–11.
5. Shaik MS, Chatterjee A, Jackson T, Singh M. Enhancement of antitumor activity of docetaxel by celecoxib in lung tumors. Int J Cancer. 2006;118(2):396–404.
6. Hida T, Kozaki K, Ito H, Miyaishi O, Tatematsu Y, Suzuki T, *et al.* Significant growth inhibition of human lung cancer cells both *in vitro* and *in vivo* by the combined use of a selective cyclooxygenase 2 inhibitor, JTE-522, and conventional anticancer agents. Clin Cancer Res. 2002;8(7):2443–7.
7. Nawrocki ST, Sweeney-Gotsch B, Takamori R, McConkey DJ. The proteasome inhibitor bortezomib enhances the activity of docetaxel in orthotopic human pancreatic tumor xenografts. Mol Cancer Ther. 2004;3(1):59–70.
8. Sweeney CJ, Mehrotra S, Sadaria MR, Kumar S, Shortle NH, Roman Y, *et al.* The sesquiterpene lactone parthenolide in combination with docetaxel reduces metastasis and improves survival in a xenograft model of breast cancer. Mol Cancer Ther. 2005;4(6):1004–12.
9. Fulzele SV, Chatterjee A, Shaik MS, Jackson T, Singh M. Inhalation delivery and anti-tumor activity of celecoxib in human orthotopic non-small cell lung cancer xenograft model. Pharm Res. 2006;23(9):2094–106.
10. Patlolla RR, Chougule M, Patel AR, Jackson T, Tata PN, Singh M. Formulation, characterization and pulmonary deposition of nebulized celecoxib encapsulated nanostructured lipid carriers. J Control Release. 2010;144(2):233–41.
11. Walker Jr JE, Odden AR, Jeyaseelan S, Zhang P, Bagby GJ, Nelson S, *et al.* Ethanol exposure impairs LPS-induced pulmonary LIX expression: alveolar epithelial cell dysfunction as a consequence of acute intoxication. Alcohol Clin Exp Res. 2009;33 (2):357–65.
12. Pardeike J, Hommoss A, Muller RH. Lipid nanoparticles (SLN, NLC) in cosmetic and pharmaceutical dermal products. Int J Pharm. 2009;366(1–2):170–84.
13. Mehnert W, Mader K. Solid lipid nanoparticles: production, characterization and applications. Adv Drug Deliv Rev. 2001;47(2–3):165–96.
14. Muller RH, Radtke M, Wissing SA. Nanostructured lipid matrices for improved microencapsulation of drugs. Int J Pharm. 2002;242 (1–2):121–8.
15. Ichite N, Chougule MB, Jackson T, Fulzele SV, Safe S, Singh M. Enhancement of docetaxel anticancer activity by a novel diindolylmethane compound in human non-small cell lung cancer. Clin Cancer Res. 2009;15(2):543–52.
16. Menendez JA, del Mar Barbacid M, Montero S, Sevilla E, Escrich E, Solanas M, *et al.* Effects of gamma-linolenic acid and oleic acid on paclitaxel cytotoxicity in human breast cancer cells. Eur J Cancer. 2001;37(3):402–13.
17. Ichite N, Chougule M, Patel AR, Jackson T, Safe S, Singh M. Inhalation delivery of a novel diindolylmethane derivative for the treatment of lung cancer. Mol Cancer Ther. 2010;9(11):3003–14.
18. Bonvillain RW, Danchuk S, Sullivan DE, Betancourt AM, Semon JA, Eagle ME, *et al.* A nonhuman primate model of lung regeneration: detergent-mediated decellularization and initial *in vitro* recellularization with mesenchymal stem cells. Tissue Eng Part A. 2012;18(23–24):2437–52.
19. Zhou C, Zhong Q, Rhodes LV, Townley I, Bratton MR, Zhang Q, *et al.* Proteomic analysis of acquired tamoxifen resistance in MCF-7 cells reveals expression signatures associated with enhanced migration. Breast Cancer Res. 2012;14(2):R45.
20. Gavina M, Luciani A, Villella VR, Esposito S, Ferrari E, Bressani I, *et al.* Nebulized hyaluronan ameliorates lung inflammation in cystic fibrosis mice. Pediatr Pulmonol. 2012. doi:10.1002/ppul.22637.
21. Tseng CL, Wu SY, Wang WH, Peng CL, Lin FH, Lin CC, *et al.* Targeting efficiency and biodistribution of biotinylated-EGF-conjugated gelatin nanoparticles administered *via* aerosol delivery in nude mice with lung cancer. Biomaterials. 2008;29(20):3014–22.
22. Guo Y, Singleton PA, Rowshan A, Gucek M, Cole RN, Graham DR, *et al.* Quantitative proteomics analysis of human endothelial cell membrane rafts: evidence of MARCKS and MRP regulation in the sphingosine 1-phosphate-induced barrier enhancement. Mol Cell Proteomics. 2007;6(4):689–96.
23. Pierce A, Unwin RD, Evans CA, Griffiths S, Carney L, Zhang L, *et al.* Eight-channel iTRAQ enables comparison of the activity of six leukemogenic tyrosine kinases. Mol Cell Proteomics. 2008;7 (5):853–63.
24. Tan HT, Tan S, Lin Q, Lim TK, Hew CL, Chung MC. Quantitative and temporal proteome analysis of butyrate-treated colorectal cancer cells. Mol Cell Proteomics. 2008;7 (6):1174–85.
25. Byron PR. Prediction of drug residence times in regions of the human respiratory tract following aerosol inhalation. J Pharm Sci. 1986;75(5):433–8.
26. De Petris L, Orre LM, Kanter L, Pernemalm M, Koyi H, Lewensohn R, *et al.* Tumor expression of S100A6 correlates with survival of patients with stage I non-small-cell lung cancer. Lung Cancer. 2009;63(3):410–7.
27. Bulk E, Hascher A, Liersch R, Mesters RM, Diederichs S, Sargin B, *et al.* Adjuvant therapy with small hairpin RNA interference prevents non-small cell lung cancer metastasis development in mice. Cancer Res. 2008;68(6):1896–904.
28. Rehbein G, Simm A, Hofmann HS, Silber RE, Bartling B. Molecular regulation of S100P in human lung adenocarcinomas. Int J Mol Med. 2008;22(1):69–77.
29. Brychtova V, Vojtesek B, Hrstka R. Anterior gradient 2: a novel player in tumor cell biology. Cancer Lett. 2011;304(1):1–7.
30. Solomon SD, McMurray JJ, Pfeffer MA, Wittes J, Fowler R, Finn P, *et al.* Cardiovascular risk associated with celecoxib in a clinical trial for colorectal adenoma prevention. N Engl J Med. 2005;352 (11):1071–80.
31. Verschraegen CF, Gilbert BE, Loyer E, Huaringa A, Walsh G, Newman RA, *et al.* Clinical evaluation of the delivery and safety of

aerosolized liposomal 9-nitro-20(s)-camptothecin in patients with advanced pulmonary malignancies. Clin Cancer Res. 2004;10(7):2319–26.
32. Latimer P, Menchaca M, Snyder RM, Yu W, Gilbert BE, Sanders BG, *et al.* Aerosol delivery of liposomal formulated paclitaxel and vitamin E analog reduces murine mammary tumor burden and metastases. Exp Biol Med (Maywood). 2009;234(10):1244–52.
33. Okamoto H, Shiraki K, Yasuda R, Danjo K, Watanabe Y. Chitosan-interferon-beta gene complex powder for inhalation treatment of lung metastasis in mice. J Control Release. 2011;150(2):187–95.
34. Zhang C, Hu W, Fang Y. 10-Hydroxycamptothecin aerosol treatment inhibits lung metastases in B16F10 melanoma mice models. Zhongguo Zhong Yao Za Zhi. 2011;36(5):618–23.
35. Garbuzenko OB, Saad M, Betigeri S, Zhang M, Vetcher AA, Soldatenkov VA, *et al.* Intratracheal *versus* intravenous liposomal delivery of siRNA, antisense oligonucleotides and anticancer drug. Pharm Res. 2009;26(2):382–94.
36. Gallo O, Franchi A, Magnelli L, Sardi I, Vannacci A, Boddi V, *et al.* Cyclooxygenase-2 pathway correlates with VEGF expression in head and neck cancer. Implications for tumor angiogenesis and metastasis. Neoplasia. 2001;3(1):53–61.
37. Eibl G, Bruemmer D, Okada Y, Duffy JP, Law RE, Reber HA, *et al.* PGE(2) is generated by specific COX-2 activity and increases VEGF production in COX-2-expressing human pancreatic cancer cells. Biochem Biophys Res Commun. 2003;306(4):887–97.
38. Tortora G, Caputo R, Damiano V, Melisi D, Bianco R, Fontanini G, *et al.* Combination of a selective cyclooxygenase-2 inhibitor with epidermal growth factor receptor tyrosine kinase inhibitor ZD1839 and protein kinase A antisense causes cooperative antitumor and antiangiogenic effect. Clin Cancer Res. 2003;9(4):1566–72.
39. Diederichs S, Bulk E, Steffen B, Ji P, Tickenbrock L, Lang K, *et al.* S100 family members and trypsinogens are predictors of distant metastasis and survival in early-stage non-small cell lung cancer. Cancer Res. 2004;64(16):5564–9.
40. Kimura K, Endo Y, Yonemura Y, Heizmann CW, Schafer BW, Watanabe Y, *et al.* Clinical significance of S100A4 and E-cadherin-related adhesion molecules in non-small cell lung cancer. Int J Oncol. 2000;16(6):1125–31.
41. Grum-Schwensen B, Klingelhofer J, Grigorian M, Almholt K, Nielsen BS, Lukanidin E, *et al.* Lung metastasis fails in MMTV-PyMT oncomice lacking S100A4 due to a T-cell deficiency in primary tumors. Cancer Res. 2010;70(3):936–47.
42. Tian T, Hao J, Xu A, Luo C, Liu C, Huang L, *et al.* Determination of metastasis-associated proteins in non-small cell lung cancer by comparative proteomic analysis. Cancer Sci. 2007;98(8):1265–74.
43. Bartling B, Rehbein G, Schmitt WD, Hofmann HS, Silber RE, Simm A. S100A2-S100P expression profile and diagnosis of non-small cell lung carcinoma: impairment by advanced tumour stages and neoadjuvant chemotherapy. Eur J Cancer. 2007;43(13):1935–43.
44. Kim RH, Peters M, Jang Y, Shi W, Pintilie M, Fletcher GC, *et al.* DJ-1, a novel regulator of the tumor suppressor PTEN. Cancer Cell. 2005;7(3):263–73.
45. Zhou Z, Kozlowski J, Schuster DP. Physiologic, biochemical, and imaging characterization of acute lung injury in mice. Am J Respir Crit Care Med. 2005;172(3):344–51.
46. Hoy A, Leininger-Muller B, Kutter D, Siest G, Visvikis S. Growing significance of myeloperoxidase in non-infectious diseases. Clin Chem Lab Med. 2002;40(1):2–8.